

# All-optical ultrafast polarization switching of terahertz radiation by impulsive molecular alignment

Min Li, Haifeng Pan, Yuqi Tong, Cheng Chen, Yi Shi, Jian Wu, and Heping Zeng\*

State Key Laboratory of Precision Spectroscopy, East China Normal University, Shanghai 200062, China

\*Corresponding author: hpzeng@phy.ecnu.edu.cn

Received June 6, 2011; revised July 29, 2011; accepted August 21, 2011;

posted August 22, 2011 (Doc. ID 148687); published September 14, 2011

We experimentally demonstrate ultrafast polarization switching of terahertz (THz) radiation generated by dual-color driving pulses composed of orthogonally polarized fundamental and second-harmonic waves, which can be controlled by field-free molecular alignment in air by modulating the relative phase between the two field components as a transient dynamic wave plate. By fine-tuning the time delay to properly match the molecular alignment revivals, a significant polarization modulation of the THz radiation is observed and both linearly and elliptically polarized THz radiations can be obtained. © 2011 Optical Society of America

OCIS codes: 320.7110, 020.2649, 190.7110.

Terahertz (THz) generation via laser filaments has attracted ever-growing attention for its high-peak field intensity and remote availability with avoided absorption of water in air [1,2]. By using two partially overlapped parallel filaments [3,4], a static electric-field-biased intense filament [5], or dual-color filaments in air [6], significant enhancement of THz radiation has been demonstrated, which could be well explained by the so-called plasma current model [1] and transition-Cherenkov electromagnetic emission [7]. As the plasma-current-based processes within dual-color filaments exhibit highly nonlinear and phase-sensitive features, the polarization of the generated THz could be controlled by adjusting the relative phase between fundamental-wave (FW) and second-harmonic (SH) pulses through changing the position of the frequency-doubling nonlinear optical crystal along the pump propagation or utilizing quartz wedges as a phase modulator [8] or using a two-plasma configuration [9]. It is of great interest to implement a THz polarization switch in an all-optical way at a remote site.

It is well known that impulsive molecular alignment [10] could induce ultrafast birefringence in air: based on this, a frequency-resolved optical gating has recently been developed for ultrafast optical imaging buffers [11]. Meanwhile, cross-phase modulation produced by field-free molecular alignment was demonstrated efficiently for remote control of intense femtosecond filaments [12,13]. Some unique effects have already been revealed in molecular alignment-mediated THz generation driven by dual-color filaments in air [14]. In this Letter, we demonstrate that prealigned molecules could function as controllable ultrafast polarization switching of the THz radiation driven by dual-color pulses. The dual-color pulses were experimentally arranged to interact with the aligned molecules before THz generation, so that we could investigate clearly the unique effects of molecular alignment-induced birefringence on the THz polarization control.

In our experiment, a 35 fs output from a Ti:sapphire laser amplifier at 800 nm of 1 kHz repetition rate was split by a 2:1 beam splitter into two beams. The weak beam

was taken as the impulsive pump pulse (M-pulse) to create molecular alignment around its focus. The strong beam (dual-color) was used to produce the FW and SH dual-color driving laser field for THz pulse generation (see Fig. 1). The FW was horizontally polarized, while the SH wave was vertically polarized. A motorizing translation stage was fixed in the pump arm to tune the time delay, and the negative time delay represented the dual-color driving pulse temporally ahead of the M-pulse. We generated the dual-color pulse by focusing the FW across a type-I  $\beta$ -BBO crystal with a lens of  $f = 50$  cm, which was followed by an  $x$ -cut 3 mm thick  $\alpha$ -BBO crystal to compensate for the phase lag between FW and SH pulses in propagation. The M-pulse was focused by a positive lens ( $f = 60$  cm), and its polarization was fixed orthogonally to that of the FW component of the dual-color pulse before the two beams were combined by a thin film polarizer (TFP). The FW, SH, and M-pulse energies were measured as 1.70, 0.27, and 0.43 mJ, respectively. The focusing position of the M-pulse was about 7 cm before that of the dual-color driving pulse. THz generation took place in the region without molecular alignment, its polarization and intensity could be readily controlled by adjusting the FW-SH phase difference via molecular alignment at remote sites without complicated interference from alignment spatiotemporal modulations [14]. After a 3 mm thick piece of Teflon to block the dual-color and aligning pulses, THz radiation was collected and focused into a 1.5 mm thick (110)-cut ZnTe crystal by two gold-coated parabolic mirrors, and a wire grid was inserted to ascertain the THz polarization state. First we measured the THz electric field parallel to the polarization

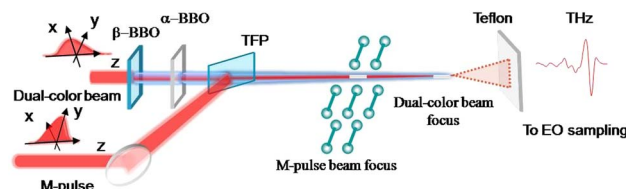


Fig. 1. (Color online) Schematic for THz polarization switching by molecular alignment. The electric-optical (EO) sampling technique was used to detect THz radiation.

of the SH wave. As the dual-color pulse was delayed around different revivals, THz generation exhibited a distinct dependence on the FW-SH phase delay. As shown in Fig. 2(a), the THz intensity influenced by the molecular alignment experienced similar periodic modulation with the alignment signals, where positive signals refer to molecular alignment parallel to the SH polarization (perpendicular to the FW polarization). Alignment-induced birefringence caused the FW-SH phase shift

$$\Delta\phi = 2\pi(\delta n_{\text{FW}}/\lambda_{\text{FW}} - \delta n_{\text{SH}}/\lambda_{\text{SH}})d, \quad (1)$$

where  $\delta n$  is the refractive index change caused by molecular alignment and  $d$  is the distance the dual-color driving pulse passing through aligned molecules, corresponding to the interaction length between the dual-color driving and M-pulse beams before THz generation around the dual-color focusing region. As molecules were parallel aligned to the SH polarization, the SH and FW components experienced, respectively, an increased and decreased refractive index, resulting in a net increase of  $\Delta\phi$ . Oppositely, as molecules were perpendicularly aligned to the SH polarization, the phase delay  $\Delta\phi$  decreased. Figures 2(b) and 2(c) show the THz intensity changes around quarter- and half-molecular-revivals, respectively. As THz radiated mainly around the dual-color pulse focus,  $\sim 7$  cm ahead of the aligning region, the

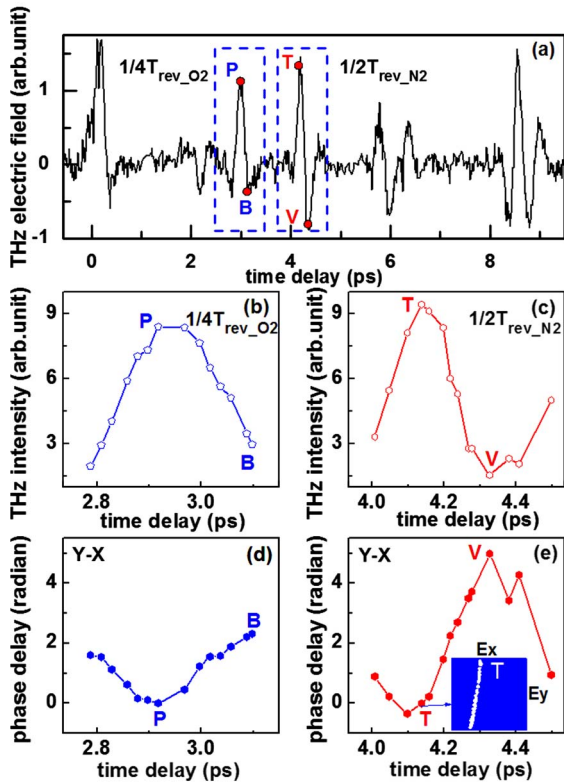


Fig. 2. (Color online) (a) Measured THz electric field from the orthogonally polarized dual-color pulse as a function of the M-pulse time delay with M-pulse energy of  $\sim 0.43$  mJ. THz intensities around (b) quarter- and (c) half-revivals. Phase delay between vertical and horizontal polarization of the THz radiation around (d) quarter- and (e) half-revivals. Y and X present the vertical and horizontal polarizations. At point T, linearly polarized THz radiation was generated.

aligned molecules could merely change the FW-SH phase delay to affect the THz generation. In our experiment, the SH was ahead of FW due to insufficient compensation provided by the 3 mm thick  $\alpha$ -BBO crystal. This was balanced by the alignment-induced FW-SH phase delay  $\Delta\phi$ . The THz intensity was optimized as the net phase delay reached zero; i.e., the FW-SH group velocity delay was completely balanced by  $\Delta\phi$ .

Interestingly, the generated THz radiation consisted of vertically and horizontally polarized components, with its polarization parallel to the FW and SH polarizations, respectively. An arbitrary phase delay between the vertical and horizontal polarization components of the THz radiation could be attained by cross-phase modulation originated from the field-free molecular alignment. Phase delays between vertically and horizontally polarized components of the THz radiation are plotted in Figs. 2(d) and 2(e), with the positive delay accounting for the horizontal polarization ahead of the vertical polarization. In accordance with different relative phases of THz components, both linearly and elliptically polarized THz radiation could be generated. As shown in Fig. 2(e), linearly polarized THz radiation was generated at point T with the highest intensity as two orthogonal THz polarization components had nearly zero phase delay. Here, we characterize the polarization state of THz radiation using the angle  $\alpha$  between the major axis of THz polarization and the  $x$  axis (parallel to the horizontal polarization), which can be written as

$$2\alpha = \arctan[2E_x E_y \cos \Delta\psi / (E_x^2 - E_y^2)], \quad (2)$$

where  $E_x$  and  $E_y$  are the electric field components of THz radiation parallel and perpendicular to  $x$  axis, respectively; and  $\Delta\psi$  is the phase delay between vertical and horizontal polarizations of the THz radiation. Prealigned molecules altered the FW-SH phase delay, which contributed to the rotation of THz polarization by changing the phase delay between the vertically and horizontally polarized components. Figure 3 shows that molecular

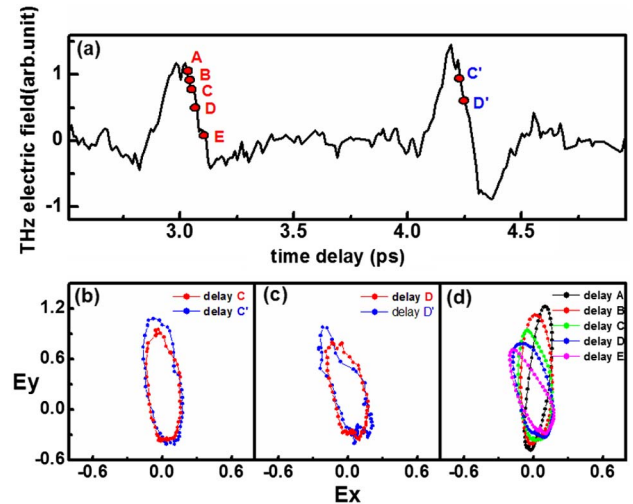


Fig. 3. (Color online) (a) Different time delays were chosen to measure THz polarizations. (b)–(c) Various THz polarizations at delays C, C', D, and D'. (d) Various THz polarizations from delay A to E around the quarter-revival.

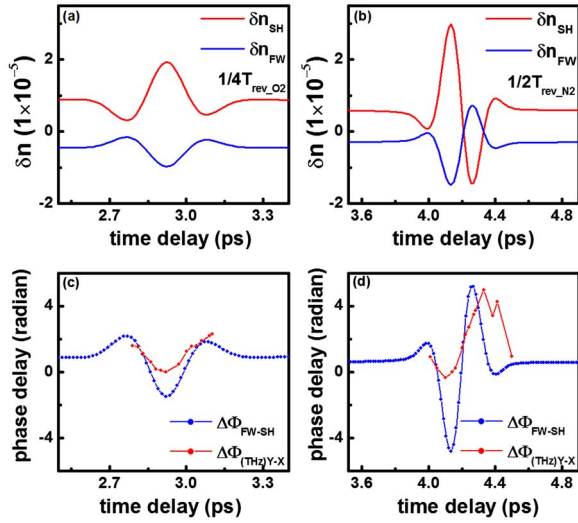


Fig. 4. (Color online) Simulated refractive index change experienced by the SH (red curve) and FW (blue curve) components around (a) quarter- and (b) half-revivals. The calculated FW-SH phase delay (blue curve) and phase delay between vertical ( $Y$ ) and horizontal ( $X$ ) polarization of the THz radiation (red curve) around (c) quarter- and (d) half-revivals, respectively.

alignment could be used as a transient wave plate to generate various spindle directions of THz polarization with different molecular alignment revivals. The phase delay between the FW and SH wave decreased at the rising edge and increased at the falling edge of THz electric field in Fig. 3(a), and the phase delay of the THz components had a similar periodic modulation, whose cosine is inversely proportional to  $\alpha$ . The phase delay between vertical and horizontal polarization components of the THz radiation was smaller at point C than at point D, and  $\alpha$  should be bigger at point D than at point C, so the polarization of the THz radiation rotated anticlockwise [see Figs. 3(b) and 3(c)]. Similarly, the continuous time delay was tuned from A to E to generate gradient spindle directions of THz radiation polarization, as shown in Fig. 3(d). Meanwhile, the ellipticity (major axis/long axis) of the elliptically polarized THz radiation changed as the THz components' relative phase changed. It could be seen that both linearly and elliptically polarized THz radiation could be attained with different spindle directions by field-free molecular alignment.

The prealigned molecules contribute to the additional refractive index variation as

$$\delta n = 2\pi\rho_0\Delta\alpha[\langle\langle\cos^2\theta\rangle\rangle - 1/3]/n_0, \quad (3)$$

where  $\langle\langle\cos^2\theta\rangle\rangle$  is the molecular alignment degree,  $\rho_0$  is the initial molecules density,  $\Delta\alpha$  is the polarizability difference,  $\theta$  is the angle between the molecule axis and M-pulse polarization, and  $n_0$  is the linear refractive index of randomly orientated molecules. In our experiment,  $\rho_0 \sim 2.5 \times 10^{19} \text{ cm}^{-3}$ ,  $\Delta\alpha \sim 1.0 \text{ \AA}^3$  (electrostatic units) for  $\text{N}_2$ ,  $\sim 1.5 \text{ \AA}^3$  for  $\text{O}_2$  and  $n_0 \sim 1$  for air. Because

the molecular alignment degree experienced by the parallel polarized field component is twice that of the perpendicularly polarized one, the additional refractive index experienced by orthogonally polarized FW and SH components is different. Figures 4(a) and 4(b) show the simulated refractive index change of the FW and SH components of the dual-color pulse around the quarter- and half-revivals of molecular air for an M-pulse intensity of  $I_M \sim 5 \times 10^{13} \text{ W/cm}^2$ . Figures 4(c) and 4(d) (blue symbols) show the corresponding phase delay between the FW and SH components of the dual-color pulse induced by the molecular alignment. The experimental results indicated that phase delays (red symbols) of two polarization components of THz radiation changed since the relative phases of dual-color pulse were modulated and exhibited a periodic modulation similar to the molecular alignment revivals.

In conclusion, we have demonstrated all-optical ultrafast polarization switching of THz radiation based on molecular alignment in air. The molecular alignment cycle determined that ultrafast switching of the THz polarization could be realized in the femtosecond scale, and the impulsive molecular alignment in air made a possible way to remotely control the polarization of the THz radiation, both of which would give us a broad field of view in many new applications of THz radiation.

This work was partly funded by the National Key Project for Basic Research (2011CB808105).

## References

1. K. Y. Kim, A. J. Taylor, J. H. Glowina, and G. Rodriguez, *Nat. Photon.* **2**, 605 (2008).
2. J. Dai, X. Xie, and X.-C. Zhang, *Appl. Phys. Lett.* **91**, 211102 (2007).
3. Y. Liu, A. Houard, B. Prade, S. Akturk, A. Mysyrowicz, and V. T. Tikhonchuk, *Phys. Rev. Lett.* **99**, 135002 (2007).
4. M. Durand, Y. Liu, A. Houard, and A. Mysyrowicz, *Opt. Lett.* **35**, 1710 (2010).
5. A. Houard, Y. Liu, B. Prade, V. T. Tikhonchuk, and A. Mysyrowicz, *Phys. Rev. Lett.* **100**, 255006 (2008).
6. D. J. Cook and R. M. Hochstrasser, *Opt. Lett.* **25**, 1210 (2000).
7. C. D. Amico, A. Houard, S. Akturk, Y. Liu, J. Le Bloas, M. Franco, B. Prade, A. Couairon, V. T. Tikhonchuk, and A. Mysyrowicz, *New J. Phys.* **10**, 013015 (2008).
8. J. Dai, N. Karpowicz, and X.-C. Zhang, *Phys. Rev. Lett.* **103**, 023001 (2009).
9. H. Wen, D. Daranciang, and A. M. Lindenberg, *Appl. Phys. Lett.* **96**, 161103 (2010).
10. H. Stapelfeldt and T. Seideman, *Rev. Mod. Phys.* **75**, 543 (2003).
11. J. Wu, P. Lu, J. Liu, H. Li, H. Pan, and H. Zeng, *Appl. Phys. Lett.* **97**, 161106 (2010).
12. S. Varma, Y.-H. Chen, and H. M. Milchberg, *Phys. Rev. Lett.* **101**, 205001 (2008).
13. H. Cai, J. Wu, A. Couairon, and H. Zeng, *Opt. Lett.* **34**, 827 (2009).
14. J. Wu, Y. Tong, M. Li, H. Pan and H. Zeng, *Phys. Rev. A* **82**, 053416 (2010).